

Hydrogen sorption properties for surface treated MgH_2 and Mg_2Ni alloys

R. Janot^a, X. Darok^a, A. Rougier^a, L. Aymard^{a,*}, G.A. Nazri^b, J.-M. Tarascon^a

^a *Laboratoire de Réactivité et Chimie des Solides, UMR 6007 Université de Picardie Jules Verne, 33 rue St Leu, 80039 Amiens, Cedex, France*

^b *General Motors, R&D, Warren, Michigan, USA*

Received 4 June 2004; accepted 21 January 2005

Available online 20 July 2005

Abstract

In our group, strong enhancement of the hydrogen sorption capacities and kinetics of Mg and intermetallic alloys was recently achieved by surface treatments using physical and chemical means separately or in convert. In the latter, our approach consists in the preparation of tailor-made composites by ball-milling the alloy with preground graphite using specific milling conditions, followed by the deposition of Pd nanoparticles on the alloys surface using the polyol process. The benefit of graphite was ascribed to the carbon coating leading to the protection of the reactive metallic particles toward oxidation and the reduction character of carbon cleaning the alloy surface of NiO. Finally, the fine Pd particles deposited at the metallic surface probably act as hydrogen pumps during the desorption process. By combining both techniques, a hydrogen desorption as high as 3 wt.% in 60 min at 150 °C and 6.2 wt.% in 30 min at 300 °C are obtained for surface treated Mg_2Ni alloy and MgH_2 , respectively. The latter treatment for MgH_2 is compared with the deposition of CeO_2 doped 6 at.% of Pt.

© 2005 Elsevier B.V. All rights reserved.

Keywords: Energy storage materials; Intermetallics; High energy ball milling; Mechanochemical synthesis

1. Introduction

Mg and Mg-based alloys are well-known for their high hydrogen storage capacities (up to 7.6% in weight for pure Mg), but the sorption kinetics remain slow at temperature below 250 °C [1–3]. In the case of Mg the absorption rate is the limiting step with a probability of the adsorption of a H_2 molecule of only 10^{-6} [4]. To overcome this problem catalysts have to be added to magnesium [5–8]. Mg powder is also very sensitive to the ambient atmosphere and the surface formation of Mg oxide or hydroxide has a negative effect on the sorption properties. Regarding the Mg_2Ni intermetallic alloy, its performances are limited by a slow desorption kinetics. The rate-controlling step for the desorption process is attributed to the permeability of hydrogen through the alloy surface. To improve the sorption properties of Mg and Mg based alloys ball-milling [9] is one of the promising process enabling the creation of nanostructure and numerous paths for hydrogen diffusion through grains boundaries. Nevertheless,

ball milling which consists in the repeated fracture and welding of powders particles needs a control of the fresh surface generated versus contaminations. Herein, the enhancement of the hydrogen sorption capacities and kinetics of Mg and intermetallic alloys is addressed by different types of surface treatments. Our approach consists in the preparation of tailor-made composites by ball-milling the Mg_2Ni alloy [10,11] or the Mg with preground graphite using specific milling conditions [12], followed by the deposition of Pd nanoparticles on the alloys surface using the polyol process [13,14].

2. Experimental

The Mg_2Ni alloys are prepared from Mg and Ni powders (40 μm , 99.9%, Alfa Aesar) by mechanical milling under argon atmosphere using a SPEX 8000 mixer-mill. The 50 cc stainless steel milling container is filled with a mixture of stainless steel balls of 6 and 12 mm diameter. The mass of Mg and Ni powder mixture is 5 g corresponding to a ball to powder weight ratio of 8. The $Mg_2Ni-C_{t,x}$ composites where t is the milling time of the preground carbon and x its BET

* Corresponding author. Tel.: +33 3 22 82 7574; fax: +33 3 2282 7590.

E-mail address: luc.aymard@u-picardie.fr (L. Aymard).

surface area are prepared by 2 h ball milling of the previously mechano-synthesized Mg_2Ni alloys with 10 wt.% of highly reactive carbon $\text{C}_{10,320}$. The alloys and the corresponding composites with carbon are coated by Pd using the polyol process (i.e. reduction of a metallic salt in a liquid polyol). Due to the high reactivity of the ball-milled Mg_2Ni alloys, ethylene glycol is chosen, since no $\text{Mg}(\text{OH})_2$ formation is detected when the alloys are dipped in this solvent. The Pd source consists of $\text{Pd}(\text{NO}_3)_2$, $2\text{H}_2\text{O}$ and the reduction occurs at room temperature. All the samples are coated with 5 wt.% of Pd, the content and the dispersion of Pd deposited on the alloy being determined by EDX spectroscopy. After the deposition is complete, the mixture is centrifuged and washed three times in acetone. A short ball-milling (3 h) of the Pd coated composite is then realized in order to improve the Pd/alloy interface. The Mg powder is ground using the SPEX 8000 mixer mill under 25 bar of hydrogen in the 50 cm^3 stainless steel milling container with a ball to powder weight ratio of 20 in order to produce the MgH_2 hydride. The MgH_2 obtained after 60 h is then ground with a $\text{C}_{10,320}$ carbon followed by the deposition of 5% of Pd in order to prepare a 5%Pd– MgH_2 – $\text{C}_{10,320}$ composite. The sorption performances of this composite are compared with the ones of the $\text{MgH}_2/\text{CeO}_2$ composite prepared by ball-milling 30 mn 5 wt.% of CeO_2 (doped 6 at.% of Pt) with MgH_2 . Pt-doped CeO_2 were prepared by a solution combustion method [15].

The crystallinity of the ball-milled powders is investigated by means of X-ray diffraction using a Philips PW1729 diffractometer $\text{Cu K}\alpha 1.5418\text{ \AA}$. The morphology of the particles is observed by Scanning Electronic Microscopy (Philips XL30 FEG) coupled with a EDX spectrometer (Oxford ISIS) allowing the determination of the alloy composition. The BET surface area is measured by N_2 adsorption using a Micromeritics Gemini II 2370 apparatus, after outgasing of the ball-milled powder at $100\text{ }^\circ\text{C}$ for 2 h. The hydrogen storage performances of the samples are determined by gravimetric measurements using a Hiden IGA 001 apparatus. After the powder is loaded into a quartz crucible (typically, with a sample mass of 150 mg) and heated at $150\text{ }^\circ\text{C}$ under secondary vacuum for 3 h, the sorption kinetics are measured under 10 bar and secondary vacuum on absorption and desorption processes, respectively. The relative errors on the experimental storage capacities are estimated to 5%.

3. Results

3.1. Surface treatments of Mg_2Ni with $\text{C}_{10,320}$ and 5 wt.% Pd: production of a 5%Pd– Mg_2Ni – $\text{C}_{10,320}$ composite

Fig. 1 clearly shows that the surface treatments improve the hydrogen absorption capacity of the composites to 2.3–2.8 wt.% range, in comparison to the 1.6 wt.% of the as prepared ball-milled Mg_2Ni alloy. A marked kinetic enhance-

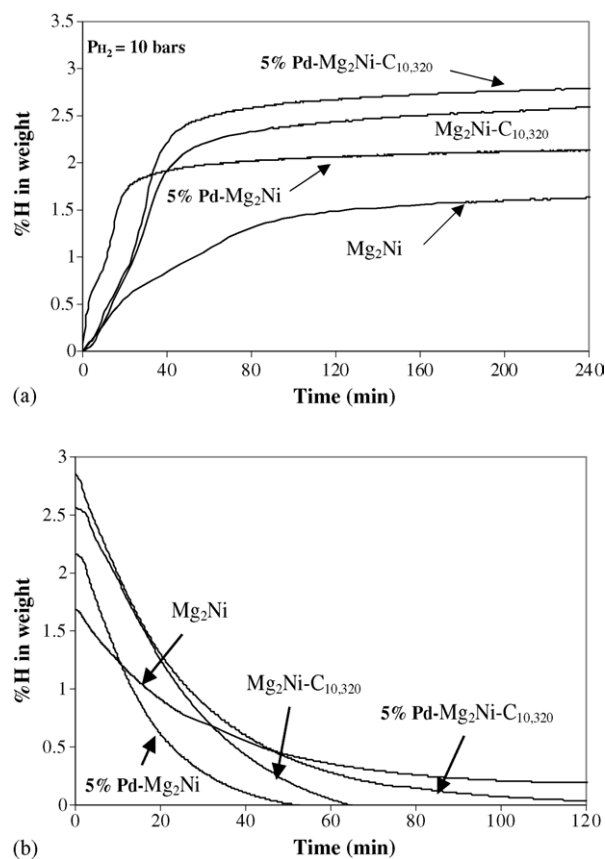


Fig. 1. Absorption (a) and desorption (b) kinetics at $150\text{ }^\circ\text{C}$ for ball-milled alloys: Mg_2Ni , 5% Pd-coated Mg_2Ni , Mg_2Ni –10% $\text{C}_{10,320}$ composite and 5% Pd– Mg_2Ni –10% $\text{C}_{10,320}$ composite.

ment is also noticed during hydrogen uptake (close to 2%) in the first 60 min. The benefit of the surface treatments is even more remarkable on the desorption process with a 2.6 wt.% hydrogen release in 60 min at $150\text{ }^\circ\text{C}$ for the Mg_2Ni – $\text{C}_{10,320}$ composite and the Pd-coated Mg_2Ni powder (cf. Fig. 1). In the case of Mg_2Ni – $\text{C}_{10,320}$ composite, the benefit in sorption kinetics and capacity is strongly linked to a high reactivity [12] of the preground carbon. Indeed, the broken graphene layers created during grinding are at the origin of the strong reducing character of carbon toward NiO oxide. So during the milling process of Mg_2Ni with $\text{C}_{10,320}$ carbon, the alloy surface is cleaned of NiO oxide contamination. The elemental analysis shows that the oxygen content of the alloy decreases from 1.4% to 0.4% after the surface treatment. As a consequence, the disappearance of the NiO barrier diffusion at the alloy surface facilitates the sorption process. The benefit of the Pd deposition on the Mg_2Ni alloy surface is high for the desorption process, showing enhanced capacity and kinetics. We speculate that during hydrogen desorption, Pd nanoparticles dispersed on the Mg_2Ni alloy surface act as hydrogen pumps [16] and therefore accelerate the migration and diffusion of hydrogen from the bulk into the Pd hydrided phase, via the grain boundaries, prior to the hydrogen desorption from Pd particles themselves.

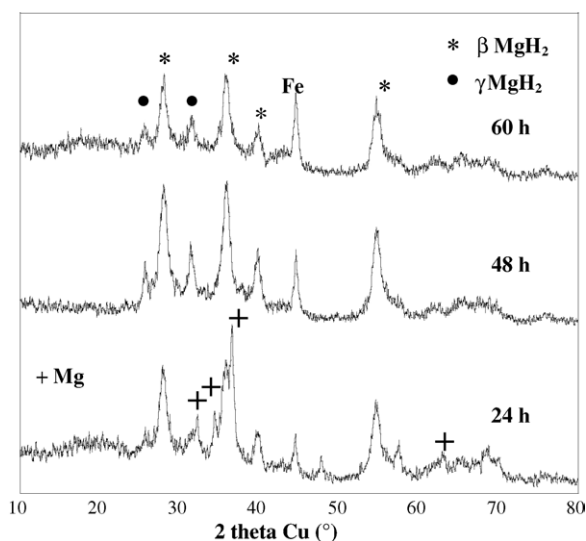


Fig. 2. XRD diagrams for MgH_2 obtained by ball-milling under hydrogen.

3.2. Synthesis and hydrogen storage performances of MgH_2 produced by grinding

A fully hydrided MgH_2 powder is obtained after 48 h of grinding since no Mg is detectable (Fig. 2). This powder is a mixture of tetragonal βMgH_2 and metastable orthorhombic γMgH_2 phases, this last being known to desorb hydrogen at temperature below that of more stable βMgH_2 [1]. From the intensities of the main reflections, the γMgH_2 content is estimated to 35% and 37% for 48 h and 60 h of milling time, respectively. The Fe impurity (detected at $44.6^\circ 2\theta$) coming from the milling tools and determined by EDX spectroscopy increases from 2 to 6 at.% between 24 and 60 h of grinding. The hydrogen desorption kinetics at 300°C under primary vacuum for the mechanothesized MgH_2 powders are presented in Fig. 3. For the 24 h ball-milled powder, the first hydrogen release is very limited (2.9 wt.% after 2 h), due to a large amount of non-hydrided Mg. The 48 and 60 h ball-milled powders desorb around 6.6 wt.% of hydrogen, a value close to the theoretical one (7.6 wt.%). The hydrogen uptake during the absorption is of the order of 6 wt.% in 120 min for all samples. From the kinetic point of view, longer is the milling time, faster is the sorption process in relation with a larger number of defects making easier the hydrogen diffusion. For the 60 h ball-milled MgH_2 20 min are sufficient to desorb 5.0 wt.% and absorb 6.0 wt.% of hydrogen.

3.3. Surface treatments of ball-milled MgH_2 with $\text{C}_{10,320}$ and 5 wt.% Pd: production of a 5%Pd- MgH_2 - $\text{C}_{10,320}$ composite

Based on the results showing the strong improvement of the hydrogen sorption kinetics of the 5%Pd- Mg_2Ni -10% $\text{C}_{10,320}$ composite, similar experiments were extended to MgH_2 . In addition the performances of the 5%Pd- MgH_2 -10% $\text{C}_{10,320}$ composite were compared with a MgH_2 -5%

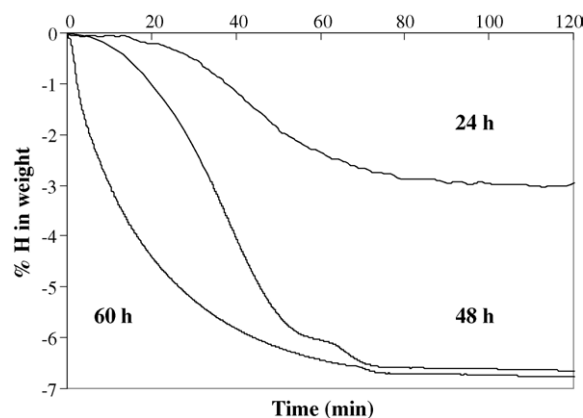


Fig. 3. Hydrogen desorption kinetics at 300°C for mechanothesized MgH_2 with milling time.

CeO_2 composite where CeO_2 is doped with 6% at of Pt. As expected, the desorption performances of the 5%Pd- MgH_2 -10% $\text{C}_{10,320}$ composite are higher than the ones of MgH_2 with 6.2 wt.% of hydrogen desorption in 30 min (Fig. 4). In this case, the benefit of graphite was ascribed to the carbon coating leading to the protection of the reactive MgH_2 particles toward oxidation whereas the metallic Pd being the driving force useful for the hydrogen diffusion. Interesting results are obtained for MgH_2 ball-milled with CeO_2 doped with 6 at.% of Pt. The hydrogen desorption rate of 5.2 wt.% in the first 15 min is higher than for the previous composite while the capacity remains slightly lower than 6 wt.% (≈ 5.7 wt.%) after 50 min. The addition of non doped CeO_2 on MgH_2 appears to be not relevant and shows that the presence of noble metal seems to play a major role in the kinetics behavior of the CeO_2 composite. Thus, the Pt and Pd role need to be distinguished due to their different nature of interaction with hydrogen. Pt does not form hydride with hydrogen but give active sites enabling a better adsorption of H_2 molecules and probably a better recombination of hydrogen atom during desorption. For Pt-doped CeO_2 samples, Pt consists, both, in Pt metallic nanoparticles dispersed onto the

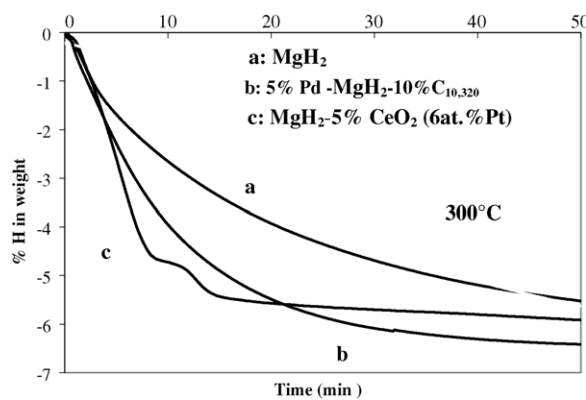


Fig. 4. First desorption kinetics at 300°C for MgH_2 ball-milled with different additives (a) MgH_2 , (b) MgH_2 + 5%Pd + 10% $\text{C}_{10,320}$, (c) MgH_2 + 5% CeO_2 (6 at.% Pt).

CeO₂ surface and in Pt²⁺ ions substituting Ce⁴⁺ in the CeO₂ matrix, creating therefore defects in the electronic structure. Such modifications of the local electronic structure of the catalyst are reported to induce enhanced activity in respect of facilitating hydrogen sorption [17]. Finally, this effect is limited at the beginning of the desorption leading to a lower capacity than the ones of the Pd hydride.

4. Conclusions

This paper reports a unique effect of the combination of two types of surface treatments with carbon and Pd on the hydrogen storage performances of mechanosynthesized Mg₂Ni alloy and MgH₂ hydride. The first approach consists in the preparation of tailor-made composites by ball-milling with preground graphite using specific milling conditions, whereas Pd-coated Mg₂Ni alloy or MgH₂ hydride are obtained by deposition of Pd nanoparticles on the powder surface using the polyol process. The starting MgH₂ is previously obtained by ball-milling of Mg powder under hydrogen. After 60 h of milling, the powder consisted in a mixture of β and γ MgH₂ phases and the first hydrogen desorption was of the order of 5.0 wt.% in 30 min at 300 °C. Finally, an hydrogen release as high as 2.8 wt.% at 150 °C is reached for a 5% Pd-coated Mg₂Ni–C_{10,320} and 6.2 wt.% in 30 min at 300 °C for the 5%Pd–MgH₂–10%C_{10,320} composite.

Current investigations, which will be reported in a forthcoming paper, show that MgH₂–C composites can show similar performances as the costly Pd-coated alloys and therefore that such composites are of great interest for applications.

References

- [1] J.J. Reilly, R.H. Wiswall, *Inorg. Chem.* 7 (1968) 2254.
- [2] E. Akiba, K. Nomura, S. Ono, S. Suda, *Int. J. Hydrogen Energy* 7 (1982) 787.
- [3] J. Huot, G. Liang, S. Boily, A. Van Neste, R. Schulz, *J. Alloys Compd.* 293–295 (1999) 495.
- [4] A.L. Reimann, *Phil. Mag.* 7 16 (1933) 673.
- [5] W. Oelerich, T. Klassen, R. Bormann, *J. Alloys Compd.* 315 (2001) 237.
- [6] Z. Dehouche, T. Klassen, W. Oelerich, J. Goyette, T.K. Bose, R. Schulz, *J. Alloys Compd.* 347 (2002) 319.
- [7] J.L. Bobet, S. Desmoulins-Kraviec, E. Grigorova, F. Cansell, B. Chevalier, *J. Alloys Compd.* 351 (2003) 217.
- [8] G. Barkhordarian, T. Klassen, R. Bormann, *J. Alloys Compd.* 364 (2004) 242.
- [9] S. Orimo, H. Fujii, *Appl. Phys. A* 72 (2001) 167.
- [10] R. Janot, L. Aymard, A. Rougier, G.A. Nazri, J.-M. Tarascon, *J. Phys. Chem. Solids* 65 (2004) 529.
- [11] R. Janot, L. Aymard, A. Rougier, G.A. Nazri, J.-M. Tarascon, *J. Mater. Res.* 18 (8) (2003) 1749.
- [12] L. Aymard, C. Lenain, L. Courvoisier, F. Salver-Disma, J.-M. Tarascon, *J. Electrochem. Soc.* 146 (1999) 2015.
- [13] F. Bonet, V. Delmas, S. Grugeon, R. Herrera-Urbina, P.Y. Silvert, K. Tekaia-Elhsissen, J.M. Tarascon, *Nano. Mater.* 11 (1999) 1277.
- [14] M.S. Hegde, D. Larcher, L. Dupont, B. Beaudoin, K. Tekaia-Elhsissen, J.-M. Tarascon, *Solid State Ionics* 93 (1996) 33.
- [15] P. Bera, A. Gayen, M.S. Hedge, N.P. Lalla, L. Spadaro, F. Frusteri, F. Arena, *J. Phys. Chem. B* 107 (2003) 6122.
- [16] R. Janot, A. Rougier, L. Aymard, C. Lenain, R. Herrera-Urbina, G.A. Nazri, J.-M. Tarascon, *J. Alloys Compd.* 356–357 (2003) 438.
- [17] W. Oelerich, T. Klassen, R. Bormann, *J. Alloys. Compd.* 322 (2001) L5–L9.